Derivation of Analytical Closed Expression for the Normalized Propagation Constant of the Multimode Buried Rectangular Optical Waveguide

Adel Zaghloul

Fuculty of Engineering , Zagazig University, Egypt
adel6730101@yahoo.com

Abstract

Simple theoretical closed algebraic expressions are derived with Hermite-Gauss trial function. These obtained expressions for the normalized propagation constant, the cut-off frequency and the field width of the slab and rectangular optical waveguides. They are shown to have reasonably good precision over a wide range of normalized frequency and modes. These closed expressions are obtained for the conventional variational method and the modified variational technique including either Maractili's method or effective index method. The derived expressions are available for the semi-infinite waveguide. Moreover, results with Hermite Gauss optical field is more confinement than cosusoidal optical field. Also in this work, we present a proposed technique to give a simple and accurate analysis of the rectangular waveguide. The proposed technique based on mixed both the first and the third methods above. The driven equations and the proposed technique show very good accuracy with respect to the finite element method, finite difference method and vectorial boundary element method.

Keywords: *Closed algebraic expression, Normalized propagation constant, Buried waveguide, Hermite Gauss and Variational method*

1. Introduction

One of the major components in all integrated optical systems is the rectangular waveguides (RW) [1, 2]. It is used in many applications such as optical power divider/combiner, couplers, filters, wavelength division multiplexer/demultiplexer and optical modulators [3, 4]. In order to be able to design efficient integrated optical devices it is important to understand the modal properties of such rectangular-core waveguides [5, 6].

The research on the waveguides has focused much attention [1-8]. Studying RW by approximate methods which are used for obtaining scalar guided modes of optical waveguides are equivalent to analyzing accurately some guide models which are more or less different [9, 10]. The modal analysis existing for the slab waveguide (SW) is extended to the RW case. The operation of the optical waveguide occurs at normalized frequency greater than the cutoff value, so the analytical methods become very good accuracy.

In this work we derived closed forms for the normalized propagation constant (b), the cut-off frequency (v_c) and the field width (D) for multimode SWs and RWs. Thus, we can understand more intuitively and clearly the parameters such may affect the normalized propagation constant and how they may enhance the optical field confinement.

Rectangular waveguides (Figure 1) was analyzed by four analytical methods which are based on the scalar variational principle using the Hermite-Gauss and cosusoidal optical fields.

i- As a whole RW by using the Variational Method (VM) [11,12].
ii- As a two SWs by using variational technique including Maractili's Method (MM) [13,14].
iii- As a two SWs by using variational technique including Effective Index Method(EIM)[13-16]
iv- As a two SWs by using Effective Width Method (EWM) [3,17].

a) Rectangular waveguide b) slab in y-direction for MM ,EIM and EWM to give (b_y) c) slab in x-direction for MM and EWM to give (b_x) d) slab in x-direction for EIM to give (b_e)

Figure 1. The Structure of the Burid Rectangular Waveguide and its Two Equivalent Slabs. N_y is the Effective Index of the Slab in y-Direction, $\mathbf{N_y^2 = n_2^2 + b_y(\,n_1^2 - n_2^2)}$

The normalized propagation constant with cosusoidal optical field is greater than that with Hermite-Gauss optical field. For single mode waveguide, Hermite Gauss optical field is sharp at the waveguide center than cosusoidal optical field.

The accuracies of these methods are very good if their numerical results are compared with those obtained by finite element method (FEM) [3], finite difference method (FDM) [18] and vectorial boundary element method (VBEM) [18].

The numerical results are done at the useful operating wavelengths (λ=1.31μm and 1.55μm).

Finally, we purpose here a simple and accurate analysis of the rectangular waveguide by mixed both VM and MM. In order to validate the proposed, the computed results are compared with those obtained from the theoretical analysis of VM.

2. Mathematical Analysis and Numerical Results with Discussions

2.1. Optical Field Analysis

The refractive indices of the waveguide (core and cladding) are very close to each other, so that the weakly guidance approximation, leading to the simplied eigenvalue problem is valid. Although the scalar wave equation can be solved by the method of separation of variables and both E^x_{pq} and E^y_{pq} modes approximately are coincides as shown in [19].

So that, the optical field distribution (Hermite Gaussian trial function [13, 17, 20]) becomes;

$$\psi_{yq}(x,y) = \psi_q(y).\psi_p(x) \tag{1.a}$$

Where

$$\psi_q(y) = A_{yq}\; S_q(y_1)\; e^{-0.5y_1^2} \tag{1.b}$$

$$\psi_p(x) = A_{xp}\, S_p(x_1)\, e^{-0.5x_1^2} \tag{1.c}$$

$$x_1 = x_1 = \sqrt{2}\, x/\alpha_{xp} \qquad \text{and} \qquad y_1 = \sqrt{2}\, y/\alpha_{yq} \quad , \tag{1.d}$$

α_{xp} and α_{yq} are the variational parameters in x and y directions, respectively, p and q are the mode numbers in x and y directions, respectively, $S_p(x_1)$ and $S_q(y_1)$ are the Hermite polynomials [17] and with the normalized power rule the values of A_{xp} and A_{yq} are;

$$A_{xp}^2 = 2^{0.5-p}/(\sqrt{\pi}\; p!\; \alpha_{xp}) \quad \text{and} \quad A_{yq}^2 = 2^{0.5-q}/(\sqrt{\pi}\; q!\; \alpha_{yq}) \tag{1.e}$$

The optical intensity (I), { $I = \psi^2(y)$ }, has (q+1) peaks (Figure 2), and the corresponding positions of theses peaks are the roots of ;

$$d\{S_q^2(y_1)e^{-y_1^2}\}/d\,y_1 = 0 \tag{2.a}$$

The maximum value of the optical intensity (I_{max}) occurs at the greatest root ($y_1=y_{1max}$) of Eq.2.a. The value of y_{1max} increases with the mode number (q) and so the position of I_{max} moves toward the edges of the optical waveguide (Figure 2).

The field width (D) is defined as the twice of the distance between the waveguide center ($y_1=0$) and the largest point of y_1 ($y_1=y_{1L}$) at which the intensity becomes e^{-1} I_{max} [4] or e^{-2} I_{max} [20].

The value of y_{1L} is the solution of;

$$S_q^2(y_{1max})e^{-y_1^2}e^{-u} = S_q^2(y_{1L})e^{-y_{1L}^2} \qquad (\text{where, } u = 1\ [4]\ \text{ or } u = 2\ [20]) \tag{2.b}$$

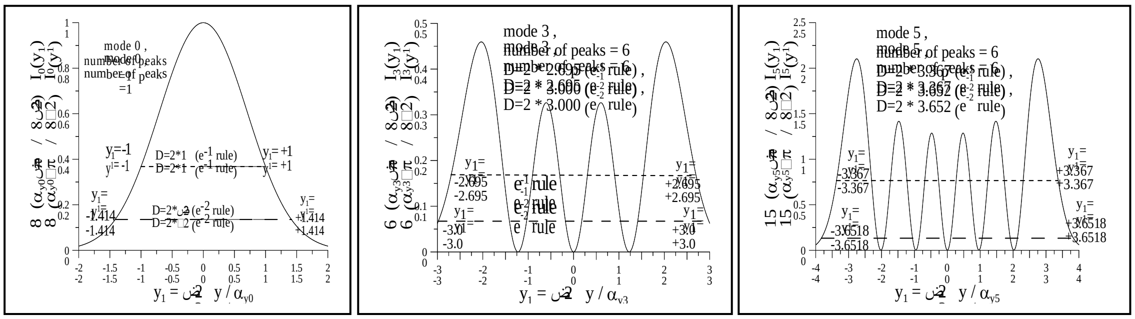

a) mode 0 b) mode 3 c) mode 5

Figure 2. Number of Optical Intensity Peaks versus Mode Number

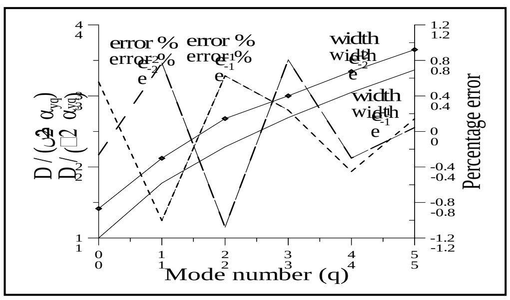

Figure 3. Field Width (D) and Percentage Error versus q

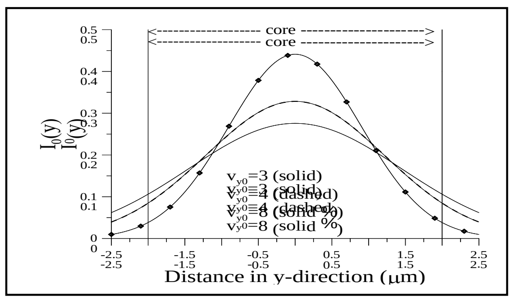

Figure 4. Dependency of the Optical Confinement on v

The values of D for the first six modes are calculated (Figure 3) and by using the fitting curve technique the relationship between D and q (with maximum percentage error ≤ 1.08 %) are;

$$D = \sqrt{2}\,\alpha_{yq}\,(1.00560952 + 0.87664603q - 0.13841905q^2 + 0.0115444q^3) \quad \text{with } e^{-1} \text{ rule}$$

$$D = \sqrt{2}\,\alpha_{yq}\,(1.41048175 + 0.86129907q - 0.14527063q^2 + 0.01254537q^3) \quad \text{with } e^{-2} \text{ rule}$$

(2.c)

Thus from Eq.2.c, the value of D increases with the mode number but it decreases with the normalized frequency (where α_{yq} decreases with the normalized frequency as indicated in Eq.3.f). Consequently as expected the optical becomes more confinement with the normalized frequency (Figure 4).

2.2. Analysis of the Slab Waveguide

2.2.1. Normalized Propagation Constant (b_{yq}) of the Slab Waveguide: The propagation constant (β_{yq}) of the slab in y-direction (Figure 1.b) with Hermite-Gaussian modal (Eq.1.b) is determined from the variational expression [11,12] as;

$$\beta_{yq}^2 = \int_{-\infty}^{\infty}\left[\psi_q(y)\,\frac{d\psi_q(y)}{dy^2} + k_o^2\,n^2(y)\psi_q^2(y)\right]dy \Big/ \int_{-\infty}^{\infty}\psi_q^2(y)\,dy \tag{3.a}$$

From Eq.1.b and the normalized power rule, the integrals in Eq.3.a become;

$$\int_{-\infty}^{\infty}\psi_q^2(y)\,dy = 1 \quad , \quad \int_{-\infty}^{\infty}[\psi_q(y)\,\frac{d\psi_q(y)}{dy^2}\,dy = -(2q+1)/\alpha_{yq} \qquad \text{and}$$

$$\int_{-\infty}^{\infty} k_o^2\,n^2(y)\,\psi_q^2(y)\,dy = k_o^2\,n_2^2 + k_o^2\,(n_1^2 - n_2^2)\int_{core}\psi_q^2(y)\,dy \tag{3.b}$$

So the normalized propagation constant (b_{yq}) is;

$$b_{yq} = -(4q+2)\,\frac{\zeta_{yq}^2}{v_{yq}^2} + \frac{2^{1-q}}{\sqrt{\pi}\;q!}\int_0^{\zeta_{yq}} S_q^2(y_1).e^{-y_1^2}\;dy_1 \tag{3.c}$$

$$= -(4q+2)\;\zeta_{yq}^2/v_{yq}^2 + R_{yq} \tag{3.d}$$

Where $k_o = 2\pi/\lambda$, v_{yq} is the normalized frequency of y-slab $\{v_{yq} = k_o T\sqrt{(n_1^2 - n_2^2)}\}$, ζ_{yq} is the normalized variational parameter of y-slab $\{\zeta_{yq} = T/\sqrt{2}\ \alpha_{yq}\}$, $b_{yq} = (\beta_{yq}^2 / k_o^2 - n_2^2)/(n_1^2 - n_2^2)$.

The relationship between v_{yq} and ζ_{yq} is defined by putting, $db/d\zeta_{yq} = 0$ as;

$$v_{yq}^2 = (4q+2)\sqrt{\pi}\;\zeta_{yq}\;e^{\zeta_{yq}^2}/\{1 + \zeta_{yq}\,F_{yq}(\zeta_{yq}) - 0.5\;dF_{yq}(\zeta_{yq})/d\,\zeta_{yq}^2\} \tag{3.e}$$

$$= (4q+2)\sqrt{\pi}\,\zeta_{yq}\;e^{\zeta_{yq}^2}\;/S_q^2(\zeta_{yq}) \tag{3.f}$$

Where

$$R_{yq} = \mathrm{erf}\left(\zeta_{yq}\right) - F_{yq}\, e^{-\zeta_{yq}^2} / \sqrt{\pi} \tag{4}$$

and F_{yq} is defined in Table 1.

As expected b_{yq} increases with v_{yq} while it decreases with the mode number (q). The corresponding, ζ_{yq} also increases with v_{yq} as shown in Figure 5.

Table 1. The Expressions of F_{yq} for Modes q = 0 → 5

q	0	1	2	3	4	5
F_{yq}	0	$+2\,\zeta_{yq}$	$+\zeta_{yq}$ $+2\,\zeta^3_{yq}$	$+2\,\zeta_{yq}$ $-(2/3)\,\zeta^3_{yq}$ $+(4/3)\,\zeta^5_{yq}$	$+(5/4)\,\zeta_{yq} + (17/6)\,\zeta^3_{yq}$ $-(5/3)\,\zeta^5_{yq} + (2/3)\,\zeta^7_{yq}$	$+2\,\zeta_{yq} - (7/6)\,\zeta^3_{yq} +$ $(53/15)\,\zeta^5_{yq} - (22/15)\,\zeta^7_{yq}$ $+ (4/15)\,\zeta^9_{y}$

2.2.2. Cutoff (v_{yqc} and ζ_{yqc}): The normalized frequency cut off (v_{yqc}) and the corresponding ζ_{yqc} are defined from Eq.3.d by putting b_{yq}=0 ;

$$v_{yqc}^2 = (4q+2) \quad \zeta_{yqc}^2 / \ \{\mathrm{erf}\left(\zeta_{yqc}\right) - \ F_{yq}\left(\zeta_{yqc}\right) e^{-\zeta_{yqc}^2}\} \tag{5.a}$$

And by mixed Eq.5.a with Eq.3.f, we obtained an equation for ζ_{yqc} as;

$$\sqrt{\pi}\,\mathrm{erf}\left(\zeta_{yqc}\right) - e^{-\zeta_{yqc}^2} \left\{F\left(\zeta_{yqc}\right) + \zeta_{yqc}\, S_q^2\left(\zeta_{yqc}\right) / \left(2^q\, q!\right)\right\} = 0 \tag{5.b}$$

Consequently the corresponding v_{yqc} is estimated from Eq.5.a.

For the first six modes vyqc and ζ_{yqc} are calculated (Figure 5.c) and from the fitting curve technique (with percentage error ≤ 1.15 %), they are;

$$v_{yqc} = 0 \qquad \text{and} \qquad \zeta_{yqc} = 0 \qquad (\text{For } q = 0) \tag{5.c}$$

$$v_{yqc} = +\,0.7930548 + 2.9947568\ q \qquad (\text{For } q \geq 1) \tag{5.d}$$

$$\zeta_{yqc} = 0.01756 + 1.09425238\ q - 0.15391429\ q^2 + 0.0108333\ q^3 \qquad (\text{For } q \geq 1) \tag{5.e}$$

The more the mode number increases, the more the values of both v_{yqc} and ζ_{yqc} increase as expected (Figure 5.c).

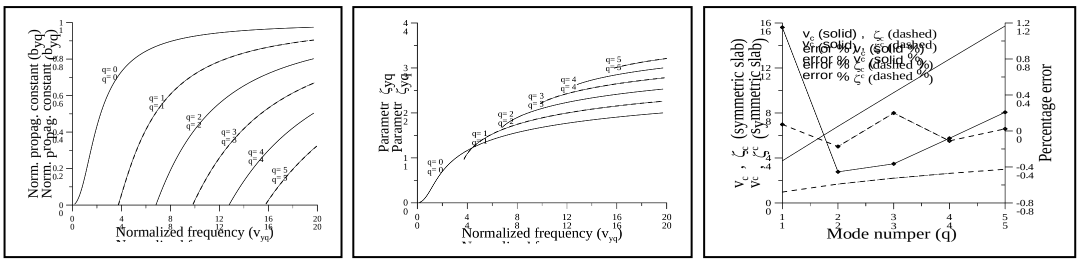

a) b_{yq} versus v_{yq} b) ζ_{yq} versus v_{yq} c) v_{yqc} and ζ_{yqc} versus q

Figure 5. Normalized Propagation Constant (b_{yq}), Normalized Variational Parameter (ζ_{yq}) and the Cut Off Values (v_{yqc} and ζ_{yqc}) for Symmetric Optical Slab Waveguide at Different Mode Number (q)

2.2.3. Semi Infinite Waveguide (y = 0 → - ∞): Which usually used with electrooptic applications. The above equations are used with the semi infinite waveguide with some modifications. $\psi_q(y)$ multiplied by factor √2, v_{yq} divided by factor 2, v_{yqc} divided by factor 2, ζ_{yq} multiplied by factor 2,and ζ_{yqc} multiplied by factor 1.

2.3. Analysis of Rectangular Waveguide

2.3.1. Variational Method (VM): With the Hermite-Gauss trial functions, The propagation constant of the rectangular optical waveguide (Fig.1) is determined by using the variational expression [11,12]

$$\beta_{VM}^2 = \frac{\iint_{-\infty}^{\infty}[\psi_{pq}(x,y)\frac{\partial^2\psi_{pq}(x,y)}{\partial x^2} + \psi_{pq}(x,y)\frac{\partial^2\psi_{pq}(x,y)}{\partial y^2} + k_o^2\, n^2(x,y)\psi_{pq}^2(x,y)]dxdy}{\iint_{-\infty}^{\infty}\psi_{pq}^2(x,y)dxdy} \quad (6.a)$$

$$= \int_{-\infty}^{\infty}\psi_p(x)\frac{d^2\psi_p(y)}{dx^2}dx \Big/ \int_{-\infty}^{\infty}\psi_p^2(x)dx + \int_{-\infty}^{\infty}\psi_q(y)\frac{d^2\psi_q(y)}{dy^2}dy \Big/ \int_{-\infty}^{\infty}\psi_q^2(y)dy + k_o^2 n_2^2$$

$$+ k_o^2(n_1^2 - n_2^2)\left[\int_{core}\psi_p^2(x)dx + \int_{core}\psi_p^2(x)dx\right] \Big/ \iint_{core}\psi_{pq}^2(x,y)dxdy \quad (6.b)$$

With the normalized power rule and from Eq.3.b, equation Eq.6.b becomes;

$$\beta_{VM}^2 = -\frac{2q+1}{\alpha_{yq}} - \frac{2p+1}{\alpha_{xp}} + \frac{2^{1-q}}{\sqrt{\pi}\,q!}\int_0^{\zeta_{yq}} S_q^2(y_1).e^{-y_1^2}dy_1 \bullet \frac{2^{1-p}}{\sqrt{\pi}\,p!}\int_0^{\zeta_{xp}} S_p^2(x_1).e^{-x_1^2}dx_1 \quad (6.c)$$

So the normalized propagation constant b_{pqVM} is;

$$b_{VM} = -(4q+2)\,\zeta_{yqVM}^2/v^2 - (4p+2)\,\zeta_{xpVM}^2/(s^2 v^2)$$

$$+ \frac{2^{1-q}}{\sqrt{\pi}\,q!}\int_0^{\zeta_{yq}} S_q^2(y_1)e^{-y_1^2}dy_1 \bullet \frac{2^{1-p}}{\sqrt{\pi}\,p!}\int_0^{\zeta_{xp}} S_p^2(x_1)e^{-x_1^2}dx_1 \quad (6.d)$$

Finally the closed form of b_{pqVM} is;

$$b_{VM} = -(4q+2)\,\zeta_{yq\,VM}^2/v^2 - (4p+2)\,\zeta_{xp\,VM}^2/(s^2 v^2) + R_{xp}\,R_{yq} \quad (6.e)$$

Where, ζ_{yqVM} ($\zeta_{yqVM} = T/\sqrt{2}\,\alpha_{yq}$) and ζ_{xpVM} ($\zeta_{xpVM} = W/\sqrt{2}\,\alpha_{xp}$) are the normalized variational parameters in x and y directions, respectively, s is the aspect ratio (s=W/T), v is the normalized frequency $\{v^2 = k_o^2 T^2(n_1^2 - n_2^2)\}$ and, R_{xp} and R_{yq} are defined from Eq.4.a by using the subscript (xp) instead of the subscript yq,

In this case, ζ_{xpVM} and ζ_{yqVM} are defined by the maximized value of b_{pqVM}, so we are obtained the following two equations.

$$v^2 = \left\{(4p+2)2^p\,p!/S_p^2(\zeta_{xpVM})\right\} \bullet \left\{\sqrt{\pi}\,\zeta_{xpVM}\,e^{\zeta_{xpVM}^2}/s^2 R_{yqVM}\right\} \quad (7.a)$$

$$v^2 = \left\{(4q+2)2^q\,q!/S_q^2(\zeta_{yqVM})\right\} \bullet \left\{\sqrt{\pi}\,\zeta_{yqVM}\,e^{\zeta_{yq\,VM}^2}/R_{xpVM}\right\} \quad (7.b)$$

The values of both ζ_{xpVM} and ζ_{yqVM} are determined by solving Eqs.7a and 7.b together.

2.3.2. Normalized Propagation Constant (b) by MM, EIM and EWM: Similarly we derived a closed form of the normalized propagation constant for both Maractilli's Method (b_{pqMM}) [13, 14], the Effective Index Method (b_{pqEIM}) [13-16] and the Effective Width Method (b_{pqEWM}) [3, 17] for the rectangular waveguide as;

$$b_{MM} = \{(4q+2)\,\zeta_{yqMM}^2/v^2 + R_{yqMM}\} + \{(4p+2)\,\zeta_{xpMM}^2/(s^2 v^2) + R_{xpMM}\} - 1 \quad (8.a)$$

$$b_{EIM} = \{(4q+2)\,\zeta^2_{yqMM}/v^2 + R_{yqMM}\} \cdot \{(4p+2)\,\zeta^2_{xpEIM}/(s^2\, v^2\, b_{yqMM}) + R_{xpEIM}\} \quad (8.b)$$

$$b_{EWM} = \{(q+1)^2\,\pi^2/(v+2)^2\} + \{(p+1)^2\,\pi^2/(s\,v+2)^2\} + 1 \quad (8.c)$$

Where, ζ_{yqMM} and ζ_{xpMM} are the normalized variational parameters for the two slabs (Figures 1.b and 1.c). ζ_{xpEIM} is the normalized variational parameter of the slab (Figure 1.d) and both R_{xpMM}, R_{xpMM} and R_{xpEIMM} are defined from Eq.4.a with replacing the subscripts (xpMM , yqMM and xpEIM) instead of subscript yq, respectively.

Figure 6 shows that the results of MM are approached with that by VM except near cutoff. But there are evidence differences between the numerical results by VM and EIM at the cutoff values. We can be noticed that b increases with s (as mentioned in [15]) and the difference between the calculated results by both MM, EIM and VM become very little (Figure 6).

2.3.3. Cutoff (v_c, ζ_{xpc} and ζ_{yqc}): They are defined From Eq.6.e by putting $b_{pqVM}=0$;

$$v^2_{cVM} = s^{-2}(4p+2)\;\; \zeta^2_{xpc} + (4q+2)\;\; \zeta^2_{yqc} \;\; / R_{xpc}\, R_{yqc} \quad (9.a)$$

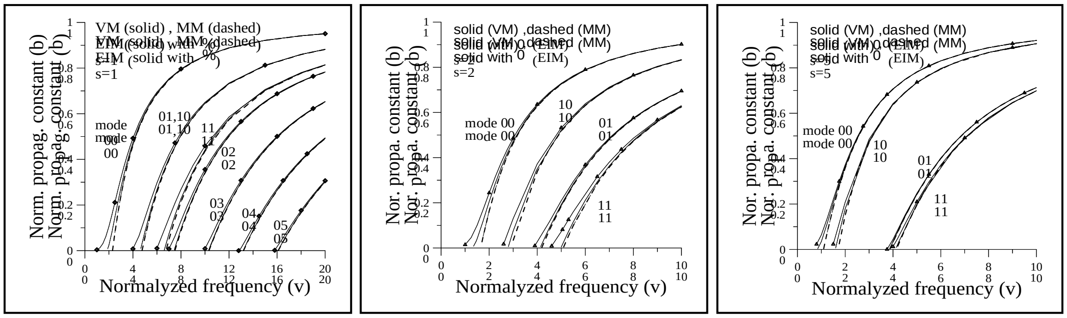

Figure 6. Comparison between VM, MM and EIM with Different Values of q and s

And the cut off values of ζ^2_{xpc} and ζ^2_{yqc} are determined by solving;

$$\{(4p+2)2^p\, p!\,\sqrt{\pi}\,\zeta_{xpc}\, e^{\zeta^2_{xpc}}\, R_{xpc}\,/S_p^2(\zeta_{xpc})\} - (4p+2)\,\zeta^2_{xpc} + s^2(4q+2)\,\zeta^2_{yqc} = 0$$

$$\{(4q+2)2^q\, q!\,\sqrt{\pi}\,\zeta_{yqc}\, e^{\zeta^2_{yqc}}\, R_{yqc}\,/S_q^2(\zeta_{yqc})\} - s^{-2}(4q+2)\,\zeta^2_{yqc} + (4p+2)\,\zeta^2_{xpc} = 0$$

The cut-off value increases with both p and q while it decreases with s as shown in Figure 7 (as stated in [15]). Effect of s becomes little at higher modes. We use v_c at s=1 as a reference of the cutoff. By using the fitting curve technique, the relationship between v_c and both p and q for s=1 (with maximum percentage error =3.32 % at p=0 with q=0 or 1, but it becomes ≤ 0.6% for the other modes) is derived as;

$$v_{cVM} = c_0 + c_1\, q + c_2\, q^2 \qquad (\text{with } s = 1) \quad (9.b)$$

Where $c_0 = 1.716881974 + 2.8552088770\, p$

$$c_1 = 2.800579958 - 0.8933905207\, p + 0.1610643837\, p^2 - 0.0119965675\, q^3$$

$$c_2 = 0.011497038 + 0.1013519959\, p - 0.0262742418\, p^2 + 0.0022088955\, q^3$$

We recommend that the cutoff by EWM can be used to find a guess value of v_{cVM}. The cutoff value by EWM (v_{cEWM}) is derived from Eq.8.c as;

$$v_{cEWM}^4 + (4s^2 + 4s)v_{cEWM}^3 + (4s^2 + 16s + 4p_1^2 - s^2q_1^2)\, v_{cEWM}^2$$

$$+(16 + 16s - 4p_1^2 - 4sq_1^2)v_{cEWM}\,(16 - 4p_1^2 - 4q_1^2) = 0 \qquad (9.c)$$

Where, $p_1 = (p+1)\pi$, $q_1 = (q+1)\pi$ and $v_{c\ EIM}$ is the positive real root of Eq.9.c.
The value of $v_{cEWM} > v_{cVM}$ (Figure 7) and $v_{cMM} > v_{cVM}$ (Figure 6) as stated in [9].

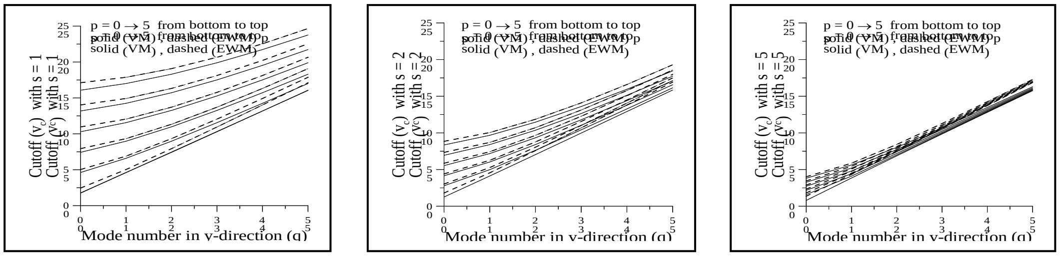

Figure 7. Cutoff Values of the Buried Rectangular Waveguide for Different Values of both p, q and s by VM (Solid) and EWM (Dashed)

2.3.4. Field Distribution: The optical field distribution is calculated from Eq.1 by using ζ_{xpMM} and ζ_{yqMM} (with MM), ζ_{yqMM} and ζ_{xpEIM} (with EIM) and ζ_{yqVM} and ζ_{xpVIM} (with VM). The optical field becomes more confinement with the aspect ratio (Figures 8) while field becomes weakly with the mode numbers (Figures 9). Because of the optical field confinement depends upon v.

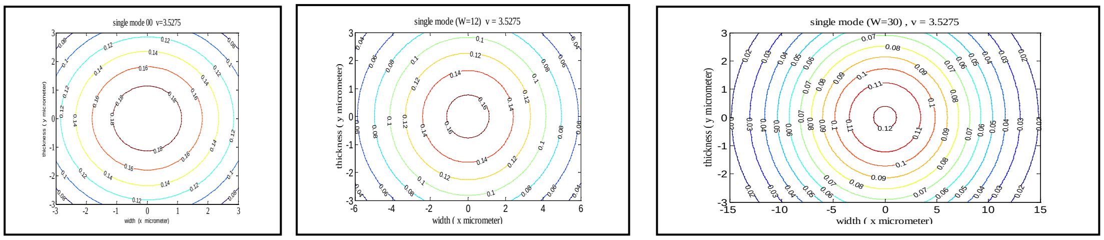

W=6 μm (s=1) W=12 μm (s=2) W=30 (s=5)

Figure 8. Field Contours for Single Mode (λ=1.31μm, T=6 μm, n_1=1.505, n_2=1.5)

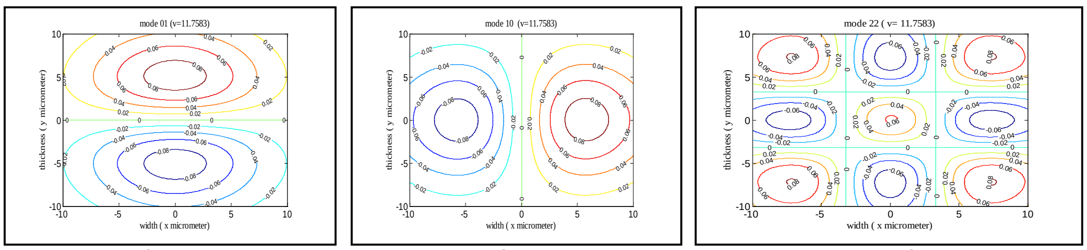

mode 01 mode 10 mode 22

Figure 9. Field Contours for Multimode (λ=1.31μm, W=T=20μm, n_1=1.505, n_2=1.5)

2.3.5. Analysis with Cosusoidal Optical Field: The rectangular waveguide is analyzed with cosusoidal optical field by MM and EIM. The normalized propagation constants of MM ($b_{MM\ cos}$) and EIM ($b_{EIM\ cos}$) and the field distribution through the core (ψ_{cos}) are derived as;

$$b_{MM\ cos} = b_y + b_x - 1 \tag{10.a}$$

$$b_{EIM\ cos} = b_e \,.\, b_y \tag{10.b}$$

$$\psi_{cos} = \cos k_x x \cdot \cos k_y y \Big/ \sqrt{\left(0.5W + 1/\gamma_x\right)\left(0.5T + 1/\gamma_y\right)} \tag{10.c}$$

Where, $k_y = (v_y/T)\sqrt{(1-b_y)}$, $\gamma_y = (v_y/T)\sqrt{b_y}$, $k_x = (v_x/W)\sqrt{(1-b_x)}$, $\gamma_x = (v_x/W)\sqrt{b_x}$

$$v_y^2 = k_0^2\, T^2 (n_1^2 - n_2^2)\ ,\ v_x = v_y\, W/T \text{ and } v_e = v_x .\, b_y\ , \tag{10.d}$$

and both b_y , b_x and b_e are the solutions of the following characteristic equations of the two slabs in y and x directions (Figures 1.b, 1.c and 1.d, respectively);

$$v_y \sqrt{1-b_y} = (q+1)\pi - 2\tan^{-1}\sqrt{-1+1/b_y} \qquad \text{(with MM and EIM)} \qquad (10.e)$$

$$v_x \sqrt{1-b_x} = (p+1)\pi - 2\tan^{-1}\sqrt{-1+1/b_x} \qquad \text{(with MM)} \qquad (10.f)$$

$$v_e \sqrt{1-b_e} = (p+1)\pi - 2\tan^{-1}\sqrt{-1+1/b_e} \qquad \text{(with EIM)} \qquad (10.g)$$

The numerical results by MM, EIM and EWM are very good accuracy if they compared with that by FEM [3] (Table 2). Where the percentage error still considered available value if it less than 5% [3].

The normalized propagation constant with cosusoidal optical field distribution is greater than that with Hermite-Gauss optical field distribution (Table 3). The field distribution of Hermite Gauss is more concentrated at the center of waveguide (Figure 8).

Table 2. Accuracy of MM, EIM, EWM and EWMap (With Cosusoidal Optical Field) by Comparison the Difference (β_{00}-β_{pq}) with that by FEM. with the Main Data Dif =10^6 (β_{00}-β_{pq}) and error % = 100 (Dif_{FEM} – Dif) / Dif

mode	10	01	20	11	21	30	12	22	40
$v_{c\ EWM}$	3.69	4.7	5.57	5.78	7.24	7.54	8.43	9.55	9.55
Dif_{FEM} [3]	2078	4111	5494	6175	9561	10145	12654	16003	15659
Dif_{MM}	2082	4116	5507	6199	9627	10177	12736	16167	15816
Dif_{EIM}	2063	4094	5450	6087	9338	10052	12367	15196	15526
Dif_{EWM}	2097	4207	5594	6306	9805	10493	13326	16830	16798
Dif_{EWMap} *	2096	4204	5590	6300	9794	10480	13307	16801	16769
R_{MM}	0.194	0.122	0.235	0.394	0.682	0.313	0.643	1.013	0.996
R_{EIM}	0.743	0.416	0.800	1.444	2.392	0.928	2.320	5.309	0.858
R_{EWM}	0.914	2.283	1.788	2.072	2.488	3.317	5.045	4.912	6.778
R_{EWMap}	0.863	2.215	1.709	1.988	2.376	3.200	3.722	4.747	6.617

* $\beta_{(EWMap)} \approx k_o n_g - 0.5 (p+1)^2 \pi^2 /\{k_o n_g W^2 (1+2/v_x)^2\} - 0.5(q+1)^2 \pi^2/\{k_o n_g T^2 (1+2/v_y)^2\}$ [3]

Table 3. Normalized Propagation Constant (b) by using MM and EIM with Hermite-Gauss and Cosusoidal Field Distributions. With the Main Data ^{1} (Hermite Gauss), ^{2} (cosusoidal), Error % = 100 ($b_{Hermite}$ – $b_{cosusoidal}$) / $b_{Hermite}$

mode	00	10	01	20	11	21
$v_{c\ EWM}$	2.02	3.69	4.7	5.57	5.78	7.24
$b_{MM}{}^1$	0.885683	0.774539	0.675891	0.369414	0.564747	0.402485
$b_{MM}{}^2$	0.896836	0.793695	0.693262	0.370841	0.590420	0.421324
error % $_{MM}$	-1.2254	-2.4732	-2.5701	-0.3863	-4.5460	-4.6807
$b_{EIM}{}^1$	0.886308	0.776850	0.678577	0.376537	0.574744	0.422788
$b_{EIM}{}^2$	0.896836	0.794951	0.694649	0.375158	0.596263	0.435878
error % $_{EIM}$	-1.1878	-2.3300	-2.3684	0.3661	-3.7442	-3.0962

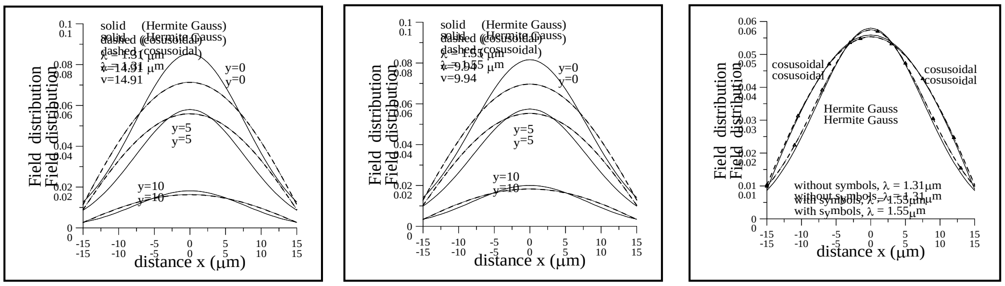

Figure 8. Comparison between Hermite Gauss and Cosusoidal Optical Field Distributions through the Rectangular Waveguide with Mode00 (W=30μm, T=20μm, n_1=1.505, n_2=1.500, with λ=1.31μm and λ=1.55μm)

3. Our Proposed Technique (Modified Variational Method, MVM)

In this proposed technique, VM is mixed with MM and so the normalized propagation constant by MVM (b_{MVM}) is evaluated from Eq.6.2 by using the variational parameters ζ_{xpMM} and ζ_{yqMM} instead of ζ_{xpVM} and ζ_{yVM}, respectively. Therefore the calculations of b_{MVM} become very simple and at the same time both MM and MVM are done together.

The accuracy of b_{MVM} becomes very good accuracy especially with higher values of the aspect ratio (Figure 11 and Table 4). Because the corresponding value of v becomes more far from cutoff.

The optical field by MVM (F_{MVM}) is calculated from Eq.1 by using ζ_{xpMM} and ζ_{yqMM}. The percentage error (R_F) between the field by VM (F_{VM}) and the field by MVM (F_{MVM}) still in the available ranges (Figure 12). With notice that at the points at which the field equals zero, the deference between F_{VM} and F_{MVM} is very small while R_F increases where the original value approaches to zero (Figure 12). Also the values of R_F% with λ=1.55μm > R_F% with λ=1.31μm (Figure 12) because of v decreases with λ. Where, R_F % =100 (F_{VM} –F_{VMV}) /F_{VM}.

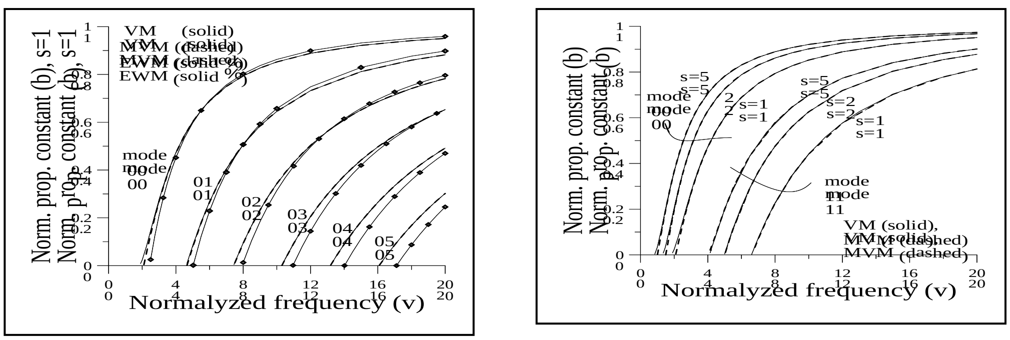

Figure 11. Comparison between VM and both MVM and EWM

Note, b_{EWM} isn't accurate especially near the cut-off values and higher modes.

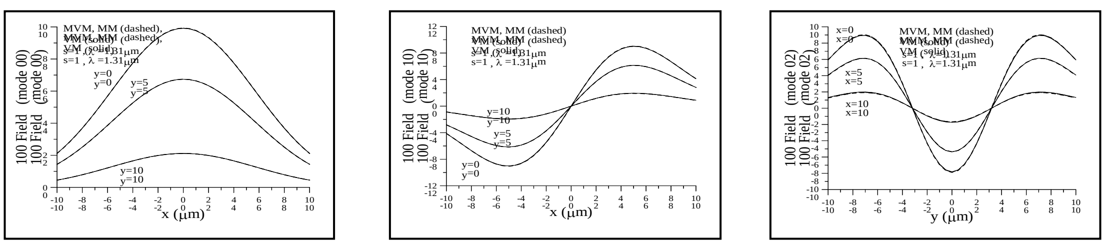

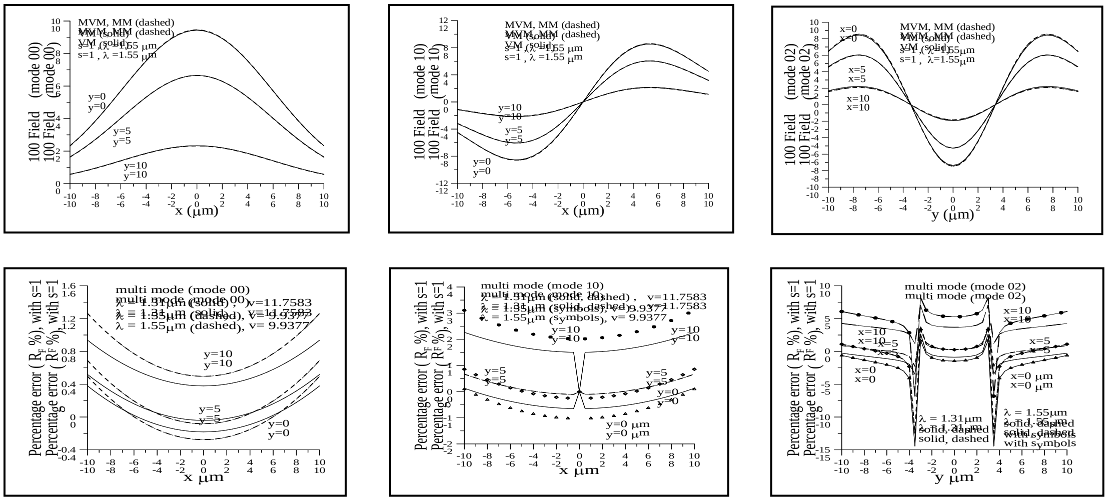

mode 00 mode 01 mode 02

Figure 12. Comparison of Field Distribution (2D) by MVM and VM at Different Values of x and y. Upper Figures (λ=1.31μm) and Middle Figures (λ=1.55μm), (W= T=20 μm, n_1=1.505, n_2=1.500)

Table 4. Percentage Error {R_b % =100 (b_{VM} –b_{VMV}) / b_{VM}}

mode	v	s = 1		s = 2		s= 5	
		v_c	R_b %	v_c	R_b %	v_c	R_b %
00	2.5	1.7759	5.00 *	1.2535	0.70	0.7928	0.080
01	5	4.6166	5.76	4.1187	0.52	3.08467	0.082
10	5	4.6166	5.76	2.7832	0.06	1.5866	0.013
11	7	6.5961	5.70	4.9836	0.14	4.1040	0.001

* R_b% ≤ 5 is considered available value [3]

To validate the methods presented above, we compare their numerical results with that published with a buried rectangular waveguide (W=0.8μm, T=0.4μm, n_1=3.52 and n_2=3.2, λ=1.15μm, p = q =0 and v=3.2048). The effective index, N =3.3137047 (FDM [18]), 3.3087656 (VBEM [18]), 3.27605(VM), 3.265596 (MM), 3.371238 (EIM), 3.362566 (EWM) and 3.367554 (MVM). And so, the percentage error (R_N%) is;R_N % =0.4195, 1.4518, 1.736, 1.4745 and 1.625 (with respect to FDM) while it becomes R_N% = 0.5694, 1.3047, 1.888, 1.6260 and 1.777 (with respect to VBEM), for VM, MM, EIM, EWM and MVM, respectively. With noticed that, the difference (n_1-n_2=0.32) does not very small. Finally, MVM is very good accurate and simple proposed.

4. Conclusion

Closed expressions have been driven for both normalized propagation constant, cutoff value and field width for the slab and the buried rectangular optical waveguides. These closed expressions are available for the semi-infinite waveguide. They are available with good accuracy over a wide range of normalized frequency and modes. A brief description of some of the common approximate methods (variational method, Maractili's method, effective index method and the effective width method) for obtaining the guided modes of an optical waveguide. The analysis has been applied with Hermite-Gauss and cosusoidal optical fields. The Hermite-Gauss optical field is sharp inside the core than that of cosusoidal.

The proposed technique is used to simplify the variational method. The driven equations and the proposed technique show very good accuracy with respect to the finite element method, finite difference method and vectorial boundary element method.

References

[1] X. Song and R. Leonhardt, "Ray-Optics Analysis of Single Mode Condition For Optical Waveguides with Rectangular-Cross-Section", Progress In Electromagnetics Research, vol. 135, **(2013)**, pp. 81-89.

[2] M. D. Davidović and M. D. Davidović, "Mode Analysis of the Optical and the Microwave Waveguides Using Electromagnetic Energy Flow Lines", Proc. of the International School and Conference on Photonics (PHOTONICA09), Acta Physica Polonica A, vol. 116, no. 4, **(2009)**, pp. 672-674.

[3] D. Khalil and A. Yehia, "Two-Dimensional Multimode Interference in Integrated Optical Structures", J. of Optics A: Pure and Applied Optics, vol. 6, no. 1, **(2004)** June, pp. 137-145.

[4] C. M. Kan and R. V. Ramaswmy, "Overlap Integral Factors in Integrated Optic Modulators and Switches", J. Lightwave Technol., vol. 7, no. 7, pp. 1063-1070, **(1989)** July.

[5] A. Kumar, K. Thyagarajan and A. K. Ghatak, "Analysis of Rectangular Core Dielectric Waveguides: An Accurate Perturbation Approach", J. Optical. Soc. American, Opt. Lett., vol. 8, no. 1, **(1983)** January, pp. 63-65.

[6] M. A. Swillam and A. S. Helmy, "Characteristics and Applications of Rectangular Waveguide in Sensing, Slow Light, and Negative Refraction", Proc. of Society of Photo-Optical Instrumentation Engineers (SPIE), Integrated Optics: Devices, Materials, and Technologies XV, San Francisco, California USA, vol. 7941, **(2011)** January 22.

[7] J. Hu and C. R. Menyuk, "Understanding leaky modes: slab waveguide revisited", Advances in Optics and Photonics 1, Optical Society of America Publisher, **(2009)** January, pp. 58-106.

[8] Sharma and A. De, "Full-Wave Analysis of Dielectric Rectangular Waveguides", Progress In Electromagnetics Research M, vol. 13, **(2010)**, pp. 121-131.

[9] A. Sharma and J.-P. Meunier, "On the scalar modal analysis of optical waveguides using approximate methods", Optics Communications, vol. 281, **(2008)**, pp. 592–599.

[10] Y. Cai, T. Mizumoto and Y. Naito, "Improved Perturbation Feedback Method for the Analysis of Rectangular Dielectric Waveguides", Lightwave Technol., vol. 9, no. 10, **(1991)** October, pp. 1231-1236.

[11] L. Piviere, A. Yi-Yan and H. Carru, "Properties of Single-Mode Optical Planar Waveguides With Gaussian Index Profile", J. Lightwave Technol., vol. LT-3, no.2, **(1985)** April, pp. 368-377.

[12] S. Gaál, "Novel Methods to Calculate Guided and Radiation Modes in Slab and Channel Waveguides", Twente University Press, Ph. D. thesis, **(2002)**, pp. 10-24.

[13] T. Rasmussen, J. Hedegaard Povlsen, A. Bjaklev, O. Lumholt, B. Pedersen and K. Rotluitt, "Detailed Comparison Of Two Approximate Methods For The Solution Of The Scalar Wave Equation For A Rectangular Optical Waveguide", Lightwave Technol., vol. 11, no. 3, **(1993)** March, pp. 429-433.

[14] K. Kawano and T. Kitoh, "Introduction to Optical Waveguide Analysis: Solving Maxwill's Equations and the Schrodinger Equation", John Wiley & Sons, Int., New-York, **(2001)**, pp. 13-52.

[15] C. R. Doerr and H. Kogelnik, "Dielectric Waveguide Theory", Lightwave Technol., vol. 26, no. 9, **(2008)** May, pp. 1176-1187.

[16] K. Iizuka, "Elements of Photonics, Volume II: For Fiber and Integrated Optics", John Wiley & Sons, Inc, **(2002)**, pp. 655-691.

[17] I. A. Erteza and J. W. Goodman, "A Scalar Variational Analysis Of Rectangular Dielectric Waveguides Using Hermite-Gaussian Model Approximations", J. Lightwave Technol., vol. 13, no. 3, **(1995)** March, pp. 493-506.

[18] T. Lu and D. Yevick, "A Vectorial Boundary Element Method Analysis of Integrated Optical Waveguides", Lightwave Technol., vol. 21, no. 8, **(2003)** August, pp. 1793-1807.

[19] H. Dong, A. Chronopoulos, J. Zou and A. Gopinath, "Vectorial Integrated Finite-Difference Analysis Of Dielectric Waveguides", Lightwave Technol, vol. 11, no. 10, **(1993)** October, pp. 1559-1564.

[20] R. Paschotta, "Encyclopedia of Lser Physics and Technology", **(2013)**.

[21] http://www.rp-photonics.com/hermite_gaussian_modes.hotmail.

Author

Adel Zaghloul Mahmoud (Assistant Professor Faculty of Engineering, Zagazig University, Egypt) was born in Sinblaween, Dakhlih Governorate, Egypt, in 1960. Received the B.Sc., M.Sc. and Ph.D scientific degrees in the Electronics and Electrical Communication Engineering, from college of engineering; B. SC. Eng. (El-Mansoura University1983), M. SC. Eng.,(El-Azhar University 1991) and Ph.D. SC. Eng. (El Menufia University,1996). His research mainly focuses on the optical waveguides, electrooptic devices and optical fibers (17 papers).